Induced Branching in Confined PbSe Nanowires

Katherine L. Hull,[†] James W. Grebinski,[‡] Thomas H. Kosel,[§] and Masaru Kuno*,[†]

Department of Chemistry and Biochemistry, Notre Dame Radiation Laboratory, and Department of Electrical Engineering, University of Notre Dame, Notre Dame, Indiana 46556

Received May 6, 2005. Revised Manuscript Received June 22, 2005

The synthesis of narrow diameter (<10 nm) straight and branched PbSe nanowires (NWs) using a seeded solution approach is described. Solution-based PbSe NWs are obtained by injecting a solution consisting of trioctylphosphine selenide (TOPSe) and Au/Bi core/shell nanoparticles (NPs) into a mixture composed primarily of a mild coordinating solvent, a fatty acid, and a Pb precursor at moderate temperatures. The resulting NWs have diameters between 5 and 10 nm and lengths ranging from 1 to 5 μm. High-resolution transmission electron microscopy (TEM) reveals that the NWs exhibit a high degree of crystallinity and grow along the ⟨100⟩ directions of the lattice. By varying the initial reaction conditions, in particular the Pb to Se precursor ratio, branched NWs can be obtained. The growth mechanism appears similar to the case of analogous (branched) CdSe NWs, although the underlying rock salt structure of PbSe leads to right angles and t-shapes as opposed to CdSe, where v-shape, y-shape, and tripod morphologies are observed due to its underlying zinc blende and wurtzite lattices. In addition, "merged-y" NWs and higher order structures exhibiting multiple branching points are observed. Both straight and branched NWs have radii well below the bulk exciton Bohr radius of PbSe (46 nm), opening up opportunities for interesting optical and electrical studies of strong confinement in this system. The current investigation also sheds additional light on the mechanism behind self-induced branching in one-dimensional (1D) nanowires.

Introduction

Recent shape control experiments, emphasizing the effects aspect ratio and morphology have on the optical and electrical properties of nanoscale materials, complement well-developed studies of quantum confinement in colloidal semiconductor nanocrystals (NCs).[1,2] In this regard, a key focus of these studies has been to adopt existing preparations for colloidal semiconductor NCs, extending them toward promoting one-dimensional (1D) and quasi zero-dimensional (0D) growth.[3] Underlying this solution-based approach to nanostructure shape control is the understanding that surfactants play an important role in controlling the morphology, growth mechanism, and even phase of low-dimensional materials.[4,5] This is underscored by the work of Peng and Alivisatos, who have actively sought a working hypothesis for the growth mechanism of CdSe in both nanoparticle (NP) and nanorod (NR) forms.[6,7] Additional quasi 0D structures such as tetrapods, recently developed for a number of II−VI materials, directly advance these shape control studies, providing different systems where the interplay among thermodynamic, kinetic, and surfactant effects can be investigated.[8−11] In each case, the all-encompassing goal has been to understand and ultimately control nanoscale crystallization.

Beyond studies associated with 0D and quasi 0D materials, there exists a need for high-quality 1D and quasi 1D structures. These systems may be used to further understand the evolution of nanoscale optical, electrical, and physical properties with size, shape, and dimensionality. The recent realization that colloidal (or laser ablated) metal NPs can be used to catalyze NW growth has been key to developing this class of materials using a variety of techniques such as vapor−liquid−solid (VLS),[12−15] solution−liquid−solid (SLS),[16,17] and supercritical-fluid−liquid−solid (SFLS) growth.[18] In all

* To whom correspondence should be addressed. E-mail: mkuno@nd.edu.
[†] Department of Chemistry and Biochemistry and Notre Dame Radiation Laboratory.
[‡] Present address: Department of Chemistry, University of Calgary.
[§] Department of Electrical Engineering.

(1) Li, J.; Wang, L. *Nano Lett.* **2003**, *3* (10), 1357.
(2) Shabaev, A.; Efros, A. L. *Nano Lett.* **2004**, *4* (10), 1821.
(3) Peng, X. G.; Manna, L.; Yang, W. D.; Wickham, J.; Scher, E.; Kadavanich, A.; Alivisatos, A. P. *Nature* **2000**, *404*, 59. Peng, Z. A.; Peng, X. G. *J. Am. Chem. Soc.* **2002**, *124*, 3343. Yu, W. W.; Wang, Y. A.; Peng, X. G. *Chem. Mater.* **2003**, *15*, 4300.
(4) Dinega, D. P.; Bawendi, M. G. *Angew. Chem., Int. Ed.* **1999**, *38* (12), 1788.
(5) Puntes, V. F.; Zanchet, D.; Erdonmez, C. K.; Alivisatos, A. P. *J. Am. Chem. Soc.* **2002**, *124*, 12874.
(6) Peng, Z. A.; Peng, X. *J. Am. Chem. Soc.* **2001**, *123*, 1389. Peng, X. *Adv. Mater.* **2003**, *15* (5), 459.
(7) Scher, E. C.; Manna, L.; Alivisatos, A. P. *Philos. Trans. R. Soc. London A* **2003**, *361*, 241.
(8) Milliron, D. J.; Hughes, S. M.; Cui, Y.; Manna, L.; Li, J.; Wang, L.; Alivisatos, A. P. *Nature* **2004**, *430*, 190. Manna, L.; Milliron, D. J.; Meisel, A.; Scher, E. C.; Alivisatos, A. P. *Nat. Mater.* **2003**, *2*, 382. Manna, L.; Scher, E. C.; Alivisatos, A. P. *J. Am. Chem. Soc.* **2000**, *122*, 12700.
(9) Jun, Y.; Lee, S.; Kang, N.; Cheon, J. *J. Am. Chem. Soc.* **2001**, *123*, 5150.
(10) Yu, W. W.; Wang, A.; Peng, X. *Chem. Mater.* **2003**, *15*, 4300.
(11) Chen, M.; Xie, Y.; Lu, J.; Xiong, Y.; Zhang, S.; Qian, Y.; Liu, X. *J. Mater. Chem.* **2002**, *12*, 748.
(12) Wagner, R. S.; Ellis, W. C. *Appl. Phys. Lett.* **1964**, *4* (5), 89.
(13) Morales, A. M.; Lieber, C. M. *Science* **1998**, *279*, 208. Lauhon, L. J.; Wang, J.; Smith, D. C.; Lieber, C. M. *Nature* **2002**, *415*, 617.
(14) Wu, Y. Y.; Yang, P. D. *J. Am. Chem. Soc.* **2000**, *123* (13), 3165. Stach, E. A.; Pauzauskie, P. J.; Kuykendall, T.; Goldberger, J.; He, R. R.; Yang, P. D. *Nano Lett.* **2003**, *3* (6), 867.
(15) Persson, A. I.; Larsson, M. W.; Stenstrom, S.; Ohlsson, B. J.; Samuelson, L.; Wallenberg, L. R. *Nat. Mater.* **2004**, *3*, 677.

10.1021/cm050952+ CCC: $30.25
Published on Web 07/30/2005

cases, high-quality straight NWs have been the end result of these syntheses. However, unlike the situation with colloidal NCs, the analogous transition from straight to branched NWs has been relatively slow, evidenced by the scarcity of reports on branching.[17,19−21] Notable progress, however, has been made very recently in terms of "higher order" structures with multiple branching points. Specific examples include branched "nanotrees" and "hyperbranched" NW structures, created by depositing catalyst NPs onto previously grown straight nanowires and applying additional VLS growth steps.[20,21] More recent studies complement these synthetic advances by providing a solution-phase approach that enables self-induced (catalyzed) NW branching. This has been demonstrated for the case of CdSe,[17] a well-developed semiconductor system in quantum dot (QD) form.

The current work further advances our understanding about solution-based NW crystallization, by describing a synthetic approach through which one can obtain not only straight but also branched PbSe NWs. A qualitative scheme for branching in this system has also been developed, complementing analogous studies on branched CdSe NWs. The ultimate goal of this and other work we have conducted is to establish a more general description of NW branching both qualitatively and quantitatively.

Whereas most NW syntheses follow VLS schemes, the PbSe NWs described here are made using a solution-based approach first introduced in the mid-1990s.[16] Common to both syntheses is the use of metal NPs to absorb precursor atoms and, in turn, to promote the asymmetric crystallization of NWs. A distinguishing feature of the solution-based or SLS approach, however, is the need for low-melting NP catalysts allowing reactions to be conducted at temperatures sustainable by solution chemistry (<400 °C).[16,17] By contrast, VLS is typically carried out at much higher temperatures (>800 °C) using gas-phase precursors.[12−15] Potential advantages of a solution-based approach include the possibility of higher yields and an increased flexibility by which the resulting NWs can be processed given their solubility in common organic solvents.[16,17] At the same time, this solubility also opens the door to future NW surface derivatization chemistries which may aid the creation of functional 1D nanostructures.

The PbSe NWs described here have diameters on the order of 5−10 nm, placing them within the strong confinement regime of the material. This occurs because the bulk exciton Bohr radius of PbSe is 46 nm.[22] Corresponding NW lengths range from 1 to 5 μm, and all NWs grow along equivalent ⟨100⟩ directions of the rock salt lattice. By varying the Pb/Se ratio used for straight NW preparations, branching can be induced in the wires. Resulting morphologies include right angles, t-shapes, and merged-y structures. The branching in these wires appears to follow a "geminate" nucleation mechanism, first described for CdSe NWs. In this scheme, multiple arms nucleate within the same NP and eventually coalesce to form a single branched wire.[17] A critical angle between the two (initially) independent arms appears to dictate whether right angles/t-shapes or merged-y structures are formed. This critical angle can be determined experimentally or estimated using simple geometric considerations. The overall branching scheme developed for PbSe appears consistent with that for CdSe and should also be applicable to other semiconductor systems. As a consequence, this generalized route to branched semiconductor nanostructures is of fundamental interest.

Experimental Section

Materials. The solvents chloroform, toluene, hexanes, and acetone were all used as received from Fisher Scientific. To prepare straight and branched PbSe NWs, trioctylphosphine (TOP, 90% Aldrich), phenyl ether (Ph_2O, 99%, Acros), Brij 30 (Acros), selenium powder (99% Aldrich), octanoic acid (98% Lancaster), and lead acetate trihydrate ($Pb(Ac)_2{\cdot}3H_2O$, 99.999% Acros) were all purchased and used as received. Solutions of trioctylphosphine selenide (TOPSe), with molarities ranging from 1 to 2.0 M, were prepared by mixing elemental Se with TOP.[23]

Au/Bi core/shell NPs used to catalyze PbSe NW growth are synthesized according to literature procedures.[17] Briefly, the Au core is made using a gold biphasic reduction procedure. The resulting particles have diameters of 1.5 nm (∼18% size distribution). The bismuth shell is subsequently created by adding $Bi(Et)_3$ to the Au NPs dispersed in a mild coordinating solvent at 100 °C. Thicker (thinner) shells are achieved by adding more (less) Bi precursor. Typical diameters of the core/shell species range from 1.4 to 3.0 nm with a ∼20% size distribution.[17] The concentration of these particles is subsequently "standardized" by matching the absorbance of the solution at 500 nm below (above) any potential Au (Bi) plasmon resonances.[17] In this manner, variations of the product yield between different NP preparations can be accounted for, leading to more reproducible NW syntheses. An estimate for the concentration of a typical Au/Bi NP preparation is ∼0.38 mM (2 mL volume).[17]

Synthesis of Straight NWs. A mixture consisting of TOP (3 mL, 6.7 mmol), Ph_2O (0.2 mL, 1.3 mmol) [or alternatively Brij 30 (0.24−0.48 mL, 0.6−1.3 mmol)], $Pb(Ac)_2{\cdot}3H_2O$ (0.02 g, 53 μmol), and octanoic acid (0.01 mL, 63 μmol) is heated to 120 °C under vacuum to dry and degas the reagents. When complete, the reaction vessel is backfilled with N_2, and the solution is heated to 175 °C. This temperature is maintained until injection of the Se precursor. In a glovebox, a solution consisting of "standardized" ∼1.4 nm diameter (30.0 μL, 0.184 mmol $BiEt_3$) Au/Bi NPs (175 μL, ∼0.067 μmol) and 1.0 M TOPSe (25.0 μL, 25.0 μmol) is prepared. This solution is then introduced into the reaction mixture at 175 °C to initiate the reaction. A dark brown/black solution is formed and is briefly kept at high temperatures (30 s−1 min) before cooling to

(16) Trentler, T. J.; Hickman, K. M.; Goel, S. C.; Viano, A. M.; Gibbons, P. C.; Buhro, W. E. *Science* **1995**, *270*, 1791. Yu, H.; Buhro, W. E. *Adv. Mater.* **2003**, *15* (5), 416. Yu, H.; Li, J. B.; Loomis, R. A.; Wang, L. W.; Buhro, W. E. *Nat. Mater.* **2003**, *2* (8), 517.
(17) Grebinski, J. W.; Richter, K. L.; Zhang, J.; Kosel, T. H.; Kuno, M. *J. Phys. Chem. B* **2004**, *108* (28), 9745. Grebinski, J. W.; Hull, K. L.; Zhang, J.; Kosel, T. H.; Kuno, M. *Chem. Mater.* **2004**, *16*, 5260.
(18) Holmes, J. D.; Johnston, K. P.; Doty, R. C.; Korgel, B. A. *Science* **2000**, *287*, 1471. Davidson, F. M., III; Schricker, A. D.; Wiacek, R. J.; Korgel, B. A. *Adv. Mater.* **2004**, *16* (7), 646.
(19) Wu, Z. H.; Mei, X.; Kim, D.; Blumin, M.; Ruda, H. E. *Appl. Phys. Lett.* **2003**, *83* (16), 3368.
(20) Wang, D.; Qian, F.; Yang, C.; Zhong, Z.; Lieber, C. M. *Nano Lett.* **2004**, *4* (5), 871.
(21) Dick, K. A.; Deppert, K.; Larsson, M. W.; Martensson, T.; Seifert, W.; Wallenberg, R.; Samuelson, L. *Nat. Mater.* **2004**, *3*, 380.
(22) Kang, I.; Wise, F. W. *J. Opt. Soc. Am. B* **1997**, *14*, 1632. Wise, F. W. *Acc. Chem. Res.* **2000**, *33*, 773.
(23) Murray, C. B.; Norris, D. J.; Bawendi, M. G. *J. Am. Chem. Soc.* **1993**, *115*, 8706.

room temperature. Chloroform is added, and the reaction mixture is centrifuged. It is then washed with acetone and/or chloroform to remove any excess surfactant.

Synthesis of Branched NWs. A mixture consisting of TOP (3 mL, 6.7 mmol), Brij 30 (0.48 mL, 1.3 mmol), $Pb(Ac)_2 \cdot 3H_2O$ (0.04 g, 105 μmol), and octanoic acid (0.02 mL, 126 μmol) is heated to 120 °C under vacuum to dry and degas the reagents. After this, the reaction vessel is backfilled with N_2 and is heated to 175 °C. In a glovebox, an injection solution consisting of "standardized" ~2.2 nm diameter (50.0 μL, 0.307 mmol $BiEt_3$) Au/Bi NPs (175 μL, ~0.067 μmol) and 1.0 M TOPSe (25.0 μL, 25.0 μmol) is prepared. This solution is then injected into the reaction mixture at 175 °C to initiate the reaction. A color change occurs whereupon the resulting branched NWs are kept at high temperatures (30 s−1 min) before being recovered in the same fashion as described above. The procedure generally yields preparations where nearly all PbSe NWs exhibit some form of branching. However, no specific shape control has been achieved with the current synthesis. Major differences from straight NW preparations include the use of larger catalyst particles and more asymmetric Pb:Se ratios (described below).

Control Experiments. To test whether straight or branched NWs can be grown without a catalyst particle, control experiments without Au/Bi NPs were conducted under the same conditions described above. In such experiments, apparent uncatalyzed NW growth was obtained in certain cases. Such wires, however, have structural differences distinguishing them from catalyzed NWs. This will be described in more detail in the Results and Discussion. Additional experiments were carried out to test whether NWs could be grown using either Pb or Se alone in the presence of Au/Bi NPs. However, no NWs were obtained in these experiments.

Instrumentation. Transmission electron microscopy (TEM) samples were prepared by dropping dilute toluene or chloroform solutions of PbSe NWs onto ultrathin carbon-coated copper grids (Ladd). Survey TEMs were conducted during the synthesis of straight and branched PbSe NWs using a JEOL JEM-100SX electron microscope. All TEM micrographs were obtained from a JEOL-2010 TEM operating at 200 kV. A Bruker D8 Advance X-ray diffractometer (Cu Kα, $\lambda = 1.54$ Å) was used to collect wide-angle X-ray diffraction (XRD) powder patterns. For either experiment, NWs were washed repeatedly with acetone and/or chloroform to remove excess surfactant. In the XRD studies, the NWs were resuspended in acetone and deposited onto a quartz single crystal (0001) off-axis substrate. Single and ensemble NW EDXS spectra were taken with a JEOL-2010 electron microscope using specimens supported on ultralight carbon substrates (Ladd). A Cliff−Lorimer algorithm was used for standardless quantification of the sample's elemental composition.

Results and Discussion

Pb chalcogenides are attractive materials that have, only recently, been intensively investigated in colloidal nanocrystal form.[22,24−32] In particular, PbSe nanostructures are potentially useful for telecommunication and sensing applications in the 1.3−1.55 μm range[29] since the room-temperature bulk band gap of PbSe (0.26 eV (~4.7 μm)[22]) enables confinement-induced tunability over a wide range of wavelengths in this region. Impact ionization has also been demonstrated in PbSe QDs making this material potentially useful in photovoltaic devices.[24] From a basic science standpoint, PbSe is an attractive material characterized by a large bulk exciton Bohr radius (46 nm), nearly identical electron and hole effective masses, and sparse electronic spectra near the band edge.[22] All facilitate a study of quantum confinement in this system.

Toward realizing both fundamental and applied interests of this material, nearly monodisperse colloidal PbSe NCs have recently been prepared through solution chemistry.[25−31] These NCs are generally grown in noncoordinating or mildly coordinating solvents such as TOP and are passivated with oleic or other fatty acids. While the overall growth temperatures are relatively low (<200 °C), the solution-based particles exhibit a high degree of crystallinity and furthermore have exceptionally high room-temperature quantum yields that approach unity (~0.8).[25−30] This suggests that colloidal Pb chalcogenide NCs, despite their low growth temperature, are generally free of internal and/or surface defects which could adversely affect their optical and electrical properties.[33] Growing interest in other nanoscale morphologies has recently led to the development of quasi 0D PbSe structures through analogous solution chemistry routes.[34] However, significant success remains to be seen in the 1D realm. Thus, the current work on straight and branched PbSe NWs begins to address this need.

Synthesis. The present method for making high-quality, quantum confined, straight and branched PbSe NWs draws from the above PbSe NC syntheses leveraging advances in the choice of precursors and coordinating/noncoordinating surfactants[25−32] with recent developments in the solution phase growth of NWs.[16,17] In particular, the choice of Pb precursor is a salt or metal oxide, which is readily coordinated with a fatty acid such as oleic acid. The actual choice of Pb precursor does not appear to affect the preparation significantly, and $Pb(Ac)_2 \cdot 3H_2O$ and PbO as well as $Pb(acac)_2$ have all been used successfully. Octanoic acid, previously employed to synthesize solution-based CdSe NWs, is used as a Pb binding species.[17] Oleic acid may also be used, although the current synthesis has been optimized for the former ligand. An apparent advantage of the metal salt/fatty acid approach is that it obviates the need for pyrophoric organometallic precursors. It also improves control over the NW synthesis since precursor decomposition rates and subsequent growth kinetics rely not on impurities in the surfactants but rather upon a deliberate choice of metal/chalcogen coordinating ligands.[36] The selection of a Se precursor is rooted in a family of stable phosphine chalco-

(24) Schaller, R. D.; Klimov, V. I. *Phys. Rev. Lett.* **2004**, *92* (18), 186601.
(25) Pietryga, J. M.; Schaller, R. D.; Werder, D.; Stewart, M. H.; Klimov, V. I.; Hollingsworth, J. A. *J. Am. Chem. Soc.* **2004**, *126* (38), 11752.
(26) Krishnan, R.; Krauss, T. D.; Harbold, J. M.; Wise, F. W.; Thomas, M. G.; Silcox, J. *Nano Lett.* **2002**, *2* (11), 1321.
(27) Wehrenberg, B. L.; Wang, C.; Guyot-Sionnest, P. *J. Phys. Chem. B* **2002**, *106*, 10634.
(28) Murray, C. B.; Sun, S.; Gaschler, W.; Doyle, H.; Betley, T. A.; Kagan, C. R. *IBM J. Res. Dev.* **2001**, *45* (1), 47.
(29) Steckel, J. S.; Coe-Sullivan, S.; Bulovic, V.; Bawendi, M. G. *Adv. Mater.* **2003**, *15* (21), 1862.
(30) Yu, W. W.; Falkner, J. C.; Shih, B. S.; Colvin, V. L. *Chem. Mater.* **2004**, *16*, 3318.
(31) Hines, M. A.; Scholes, G. D. *Adv. Mater.* **2003**, *15* (21), 1844.
(32) Sashchiuk, A.; Langof, J.; Chaim, R.; Lifshitz, E. *J. Cryst. Growth* **2002**, *240*, 431.
(33) Allan, G.; Delerue, C. *Phys. Rev. B* **2004**, *70*, 245321.
(34) Lifshitz, E.; Bashouti, M.; Kloper, V.; Kigel, A.; Eisen, M. S.; Berger, S. *Nano Lett.* **2003**, *3*, 857. Sashchiuk, A.; Amirav, L.; Bashouti, M.; Krueger, M.; Sivan, U.; Lifshitz, E. *Nano Lett.* **2004**, *4* (1), 159.

genide compounds first utilized by Steigerwald to demonstrate the synthesis of solid-state materials from molecular precursors.[37] In turn, these chalcogenide compounds have since been used to successfully synthesize high quality low dimensional II−VI materials[3,5−10,16,17,23] and are convenient systems since they are relatively easy to prepare and are air stable in many cases.

Characterizing the growth of both PbSe QDs and NWs is a strong preference for weakly coordinating surfactants such as TOP, phenyl ether, and Brij 30. While other more strongly coordinating ligands such as trioctylphosphine oxide (TOPO) or amine-based species have been successfully employed in the growth of other QD/NW systems such as CdSe, they appear to retard or even prevent the growth of PbSe nanostructures in our case. Temperatures in the NW synthesis are typically lower than 200 °C, which parallels the growth of PbSe QDs. This contrasts to CdSe and other systems where reaction temperatures are typically much higher (>300 °C). In either case (PbSe QDs or NWs), however, a crystalline product is obtained as demonstrated through PbSe NWs in HRTEM micrographs shown below. The requirement of a low growth temperature appears to be predominantly rooted in the temperature instability of the fatty acid/Pb complex which leads to a precipitation at higher temperatures. Even when growth temperatures above 200 °C have been achieved, resulting PbSe NWs generally have large diameters (>10 nm) and rough surfaces, suggesting ideal growth temperatures between 150 and 200 °C.

Optimization of the synthesis has been conducted by exploring a parameter space analogous to that described for straight/branched CdSe NWs.[17] In particular, the reaction mixture concentration, overall reaction temperature, Pb:Se ratio, catalyst NP size, and catalyst NP concentration were all varied to test whether qualitative trends developed for CdSe could be applied to PbSe. In all cases, with the exception of the branching dependence on the metal:chalcogen ratio, the trends established for CdSe appear to hold for PbSe. To illustrate, an increase in the reaction mixture concentration enables the competitive growth of PbSe QDs over NWs. Conversely, a decrease of the concentration appears to promote the uncatalyzed transverse growth of PbSe NWs, increasing their overall diameters at the expense of their length. NW growth is therefore conducted at intermediate concentrations that are empirically determined. This behavior highlights the competition between catalyzed and uncatalyzed growth in solution-based NW reactions.[17] The effects of catalyst concentration are also identical with that for CdSe.[17] In this respect, too little catalyst enables the independent nucleation of PbSe QDs to become competitive with NW growth. Conversely, too much catalyst leads to the formation of irregular Au/Bi aggregates. This latter problem appears to be more severe in PbSe than in CdSe and may ultimately limit resulting NW size distributions. An intermediate catalyst concentration, between these two extremes, is therefore used.

Temperature effects are difficult to determine given the relatively narrow range of values suitable for PbSe NW growth. However, one clear conclusion is that no strong temperature preference for straight versus branched NW growth is observed. By contrast, in CdSe, higher temperatures (>330 °C) favor the growth of straight NWs; lower temperatures (∼270 °C) favor the growth of branched NWs. This behavior was suggested as resulting from a competition between kinetic and thermodynamic effects, with a preference for the CdSe zinc blende structure over the wurtzite phase at lower temperatures.[17] In PbSe no such phase admixtures exist, potentially explaining why this apparent temperature dependence, delineating straight from branched CdSe NW growth, appears absent here.

Effects of the Au/Bi NP size (∼1.5−3 nm diameter) are generally more straightforward to interpret. Here a correlation is found between the diameter of the initial metal NP and the width of the resulting NW. In particular, small (large) particles yield thin (thick) NWs. This agrees with previous observations of a direct catalyst NP/NW diameter correlation in both VLS- and SLS-based systems.[13−17] Straight NWs are commonly made using ∼1.4 nm diameter NPs. In the case of branched NWs, slightly larger catalyst particles (2.2 nm diameter) are used, consistent with previous observations in CdSe of a NP size below which branching becomes inefficient.[17] A more thorough mapping of the NW diameter dependence with catalyst size in straight and branched preparations, however, is complicated by the tendency of the NPs to aggregate during the reaction.

By far, however, the greatest impact on either straight or branched NW growth is the metal-to-chalcogen ratio. In this respect, straight PbSe NW syntheses are conducted with initial Pb:Se ratios of 2:1. This is analogous to CdSe where an asymmetric ∼7:1 Cd:Se ratio is used to promote straight NW growth.[17] Branched PbSe NWs, however, are grown under much less stoichiometric conditions, with Pb:Se ratios reaching ∼4:1. This differs from CdSe, where a more stoichiometric Cd:Se ratio of ∼1.7:1 promotes branching.[17] Although the actual origin of the sensitivity to initial metal/chalcogen precursor ratios is not fully understood, in PbSe it may be tied to an increased nucleation rate driven by higher concentrations of either Pb or Se in solution relative to the molten catalyst. This would then lead to a higher probability for nucleating two wires on the same particle. The proposed scenario is further supported by examples where increasing the Se to Pb concentration results in a similar increase in branching. However, NWs grown under these conditions have rough surfaces, possibly originating from uncatalyzed (transverse) growth.

Straight/branched NW syntheses are therefore optimized by empirically varying all of the above parameters. The resulting straight (branched) PbSe NWs are made with 1.4 (2.2) nm diameter Au/Bi NPs at 175 °C. They have narrow diameters (5−10 nm) and grow exclusively along ⟨100⟩ directions of the underlying rock salt lattice.

An interesting point is that the initial diameter of the catalyst NP ranges from 1.4 to 3.0 nm.[17] Since the resulting PbSe NWs have significantly larger widths (5−10 nm), this suggests that the catalyst must itself increase in diameter

(35) Cho, K. S.; Talapin, D. V.; Gaschler, W.; Murray, C. B. *J. Am. Chem. Soc.* **2005**, *127*, 7140.
(36) Peng, Z. A.; Peng, X. G., *J. Am. Chem. Soc*. **2001**, *123*, 183. Qu, L. H.; Peng, Z. A.; Peng, X. G. *Nano Lett*. **2001**, *1*, 333.
(37) Steigerwald, M. L.; Sprinkle, C. R. *Organometellics* **1988**, *7*, 245.

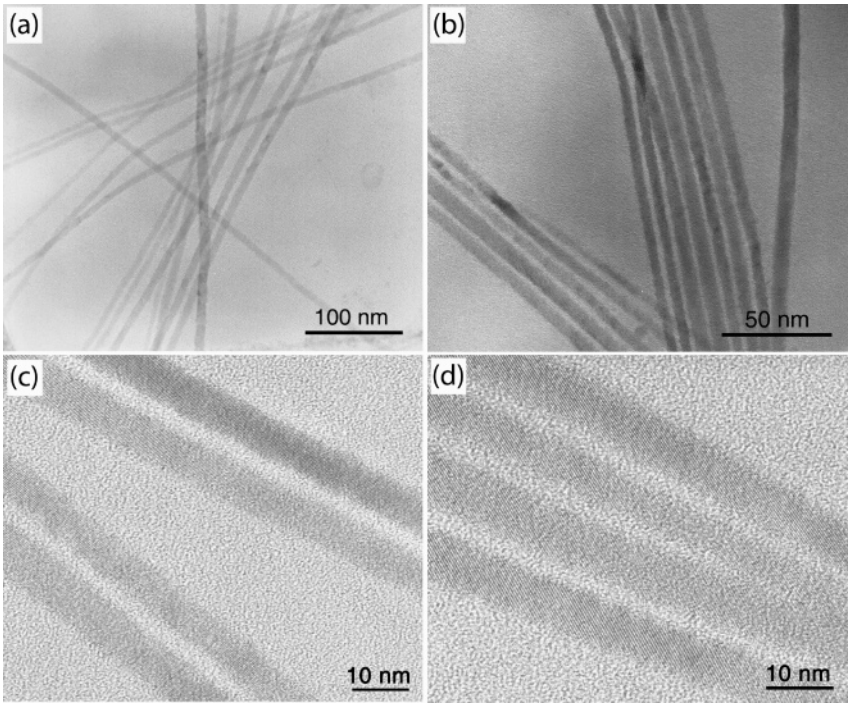

Figure 1. (a−d) Low- and high-resolution TEM micrographs of straight PbSe NWs.

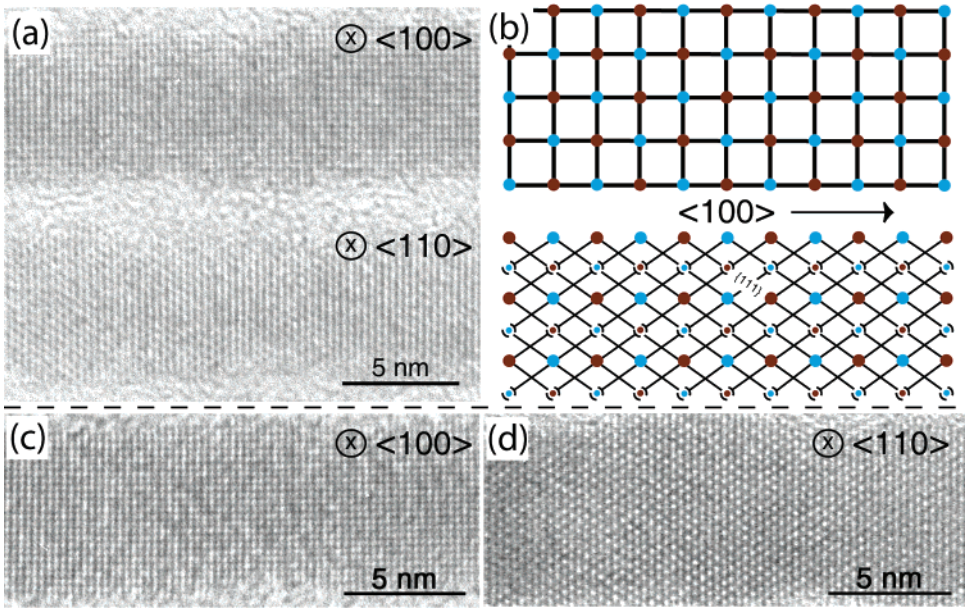

Figure 2. HRTEM of straight NWs oriented along ⟨100⟩ and ⟨110⟩ as well as corresponding cartoons.

during the reaction. The hypothesis is supported by low- and high-resolution TEM micrographs of straight NWs with catalyst particles still attached to one of their ends (Supporting Information). NP growth may therefore indicate an induction period before which supersaturation can be achieved, leading to the seeded growth of PbSe NWs. Aggregation of catalyst particles also increases the NP size. Such aggregation has been observed in our preparations and appears to be the primary effect limiting the overall narrowness of resulting NW width distributions. In more optimal cases, sections of an ensemble have size distributions as low as 12(5)%. However, larger diameter wires, presumably originating from catalyst aggregation, routinely cause the overall ensemble distribution to swell to values at or above 30%. Nevertheless, the noticeable appearance of many regions having narrow size distributions within a given ensemble suggests that further improvements in the preparation are possible. At the same time, intra-NW diameters appear fairly uniform. NW widths measured at 7 or more positions along their length indicate a 7(3)% fluctuation of the intra-NW diameter. Occasionally tapered wires are observed. Sample images used for these studies are provided in the Supporting Information.

Figure 1a,b provides examples of both the narrow diameter distributions and the uniform NW thicknesses that are possible. Furthermore all wires are crystalline and exhibit lattice fringes apparent in HRTEM images shown in Figure 1c,d as well as Figure 2. Additional TEM micrographs are provided in the Supporting Information. Thus, while these results suggest that the diameter distributions of either PbSe or CdSe NWs are ultimately influenced by the initial size

distribution of the Au/Bi catalyst (~20%),[17] the apparent growth/aggregation of the NPs during the reaction complicates any simple statement as to the primary cause of resulting width variations. Correspondingly, NW lengths in these preparations vary from 1 to 5 μm, with no strong length dependence on the reaction conditions.

PbSe NWs are generally lattice imaged in two zone axes (viewing directions) (Figure 2), ⟨100⟩ and ⟨110⟩, both normal to the ⟨100⟩ growth direction. The top of Figure 2a shows a wire viewed along the ⟨100⟩ zone axis. Under this condition, lattice fringes appear as a square pattern of {200} planes, depicted in more detail in the accompanying cartoon. Alternatively, the PbSe NWs are viewed along the ⟨110⟩ zone axis (bottom, Figure 2a). In this configuration, the wires exhibit either criss-crossed or parallel lattice fringes depending upon the exact orientation of the wire. The criss-cross fringes originate from {111} planes both 70.5 and 109.5° apart while the (vertical) parallel lattice fringes originate from {200} planes normal to the ⟨100⟩ growth axis. This is illustrated in the accompanying cartoon and in the actual HRTEM micrograph shown in Figure 2a (bottom). A measurement of fringe spacings in experimental HRTEM images supports the assignment, showing good agreement with predicted {111} and {200} *d* spacings (3.65 Å experimental versus 3.53 Å theoretical and 3.02 Å experimental versus 3.06 Å theoretical, respectively). Additional, HRTEM images of ⟨100⟩- and ⟨110⟩-oriented NWs are shown in Figure 2c,d, respectively.

Variations of the straight NW preparation, in particular the Pb:Se precursor ratio, lead to branched NWs. In general, increasing the Pb:Se ratio toward an asymmetric 4:1 limit increases the degree of catalyzed branching. Beyond this, NWs are observed to develop rough surfaces potentially due to a competition between catalyzed (longitudinal) growth and uncatalyzed (transverse) growth. This sensitivity of branching to precursor stoichiometry has also been observed with CdSe wires.[17] We speculate that it arises from the creation of conditions amenable to nucleating multiple NWs within a given catalyst particle. In this respect, the effect may be related to an increased nucleation rate driven by higher concentrations of either Pb or Se in the growth solution relative to the molten catalyst.

Two general branched morphologies are commonly observed in PbSe NWs. They are t-shapes/right angles and "merged-y's." Figure 3 provides three HRTEM images of t-shaped NWs. Occasionally wires having only a right angle are observed, but these structures ultimately originate from incomplete t-shape growth. These morphologies should be contrasted to branched CdSe tripods, v-shapes, and y-shapes.[17] Differences in the morphology originate from the underlying crystal structure of the material. Whereas rock salt is the dominant structure of PbSe, both tetrahedrally bonded zinc blende (ZB) and wurtzite (W) are the predominant phases of CdSe. As such, the growth direction of straight and branched PbSe NWs are normal to the {100} faces of the rock salt lattice. By contrast, in CdSe the preferred growth planes are the low-energy {111}/{0001} surfaces of the ZB and W crystal. This leads to structures with characteristic 109.5° angles.[17]

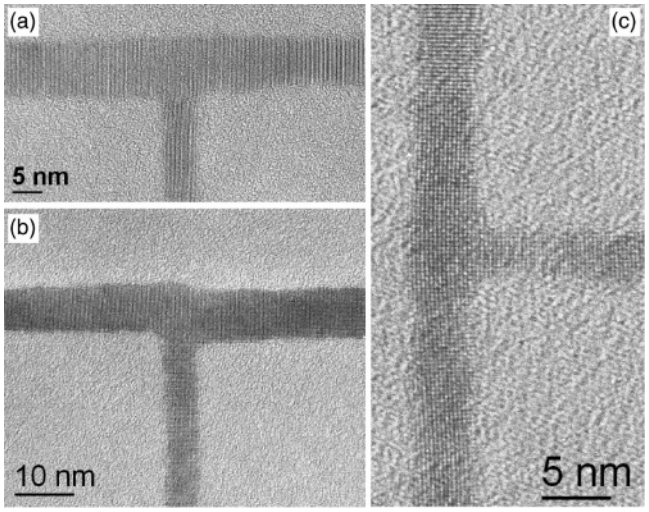

Figure 3. (a−c) High-resolution TEM micrographs of t-shape PbSe NWs.

HRTEM micrographs of t-shapes in Figure 2a,b indicate that the wires are crystalline and have smooth surfaces. T-shaped arms grow orthogonal to one another, along equivalent ⟨100⟩ directions. An average angle of 90° (σ = 1°) is measured between the arms of over 40 different t-shaped/right angle NWs. Because of their ⟨100⟩ growth directions, branched NWs naturally align themselves with a ⟨100⟩ zone axis along the viewing direction, unlike the case of straight PbSe NWs which have random orientations about their ⟨100⟩ growth axis. This is analogous to the case of branched CdSe NWs which are all ⟨110⟩ oriented.[17]

A third class of branched PbSe NW is a "merged-y" structure, consisting of two ⟨110⟩-oriented arms (α, β) fused together through a twin or grain boundary along the length of an additional "arm" denoted γ in Figure 4 (additional micrographs in Supporting Information). The interesting feature of this NW is that its structure does not appear to be unique to a given material. This was suggested earlier in a qualitative branching mechanism developed for CdSe[17] and appears to be borne out here by the appearance of similar merge-y structures. We hypothesize that such wires occur in PbSe when two arms nucleate on a given catalyst particle with a mutual angle below a critical value ($\theta_{crit} \sim 77.3°$). Under these conditions, the rapid growth of both arms prevents the wires from reorienting on a liquid NP surface until orthogonal. Instead, upon meeting, the arms accommodate each other through either a low-energy twin or a high-angle grain boundary. In the case of a low-energy twin, this results in an $-\alpha\beta$ angle of 70.5°, assuming ⟨100⟩ α,β growth directions.

The predominance of twin boundaries in merge-y NWs is explained by the fact that the twin is the lowest energy configuration possible between two single-crystal FCC grains. This should be contrasted to CdSe merge-y's where the interface is always a high-angle grain boundary.[17] Other examples of this behavior include Au or Ag nanorods, which show 5-fold twinning along the length of the rod.[38,39]

(38) Johnson, C. J.; Dujardin, E.; Davis, S. A.; Murphy, C. J.; Mann, S. *J. Mater. Chem.* **2002**, *12*, 1765.
(39) Wiley, B.; Sun, Y.; Mayers, B.; Xia, Y. *Chem.*—Eur. J. **2005**, *11*, 454.

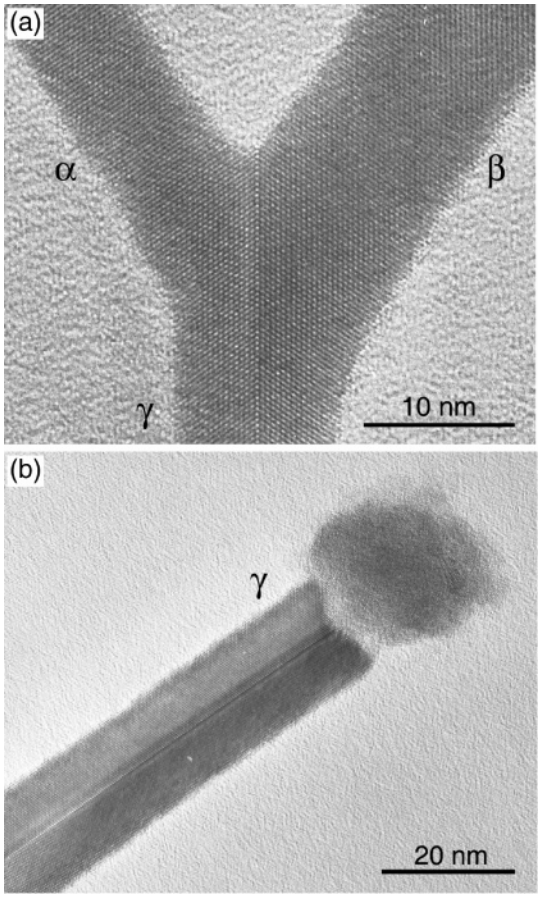

Figure 4. HRTEMs of PbSe (a) merged-y structure and (b) merged-y tip with catalyst NP.

Occasional merge-y NWs with apparent $-\alpha\beta$ angles greater than or less than 70.5° are also seen. At first glance this suggests the presence of a grain boundary. However, the angle mismatch is more likely explained by a modest offset between the actual NW arm growth direction and the idealized ⟨100⟩ growth vector. This has been established by examining lattice-resolved HRTEM images of such wires. Nonetheless, we do not exclude the occurrence of PbSe merge-y NWs with grain boundaries.

More structural information about merge-y NWs can be extracted from HRTEM micrographs. In particular, a close examination reveals that such NWs have ⟨110⟩ zone axes along the viewing direction. This configuration is induced by a twin between α and β (Figure 4). A HRTEM micrograph of the merged-y junction is shown in Figure 5 a, with an idealized cartoon of the atomic arrangement provided in Figure 5b). In all cases where lattice resolved HRTEM images are available, a {111} twin boundary runs down the center of the structure, with parallel {200} planes normal to the ⟨100⟩ growth directions of the two arms on either side. The angle between these planes forms an angle of 70.5°. Likewise, a complementary angle of 109.5° faces downward. Both values are in excellent agreement with measured $-\alpha\beta$ (complementary) angles of the merge-y NWs. The 109.5° angle between the NW tip and the catalyst particle (Figure 4b) further suggests that catalyzed growth of γ occurs by addition to low energy {100} faces. Occasionally an upward facing 140° angle will be observed in HRTEM images such as Figure 5. This is due to the angle

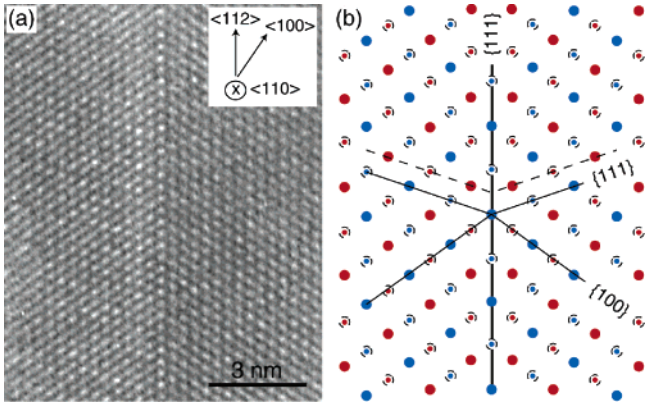

Figure 5. (a) HRTEM and (b) cartoon of twinned merged-y junction in a PbSe NW.

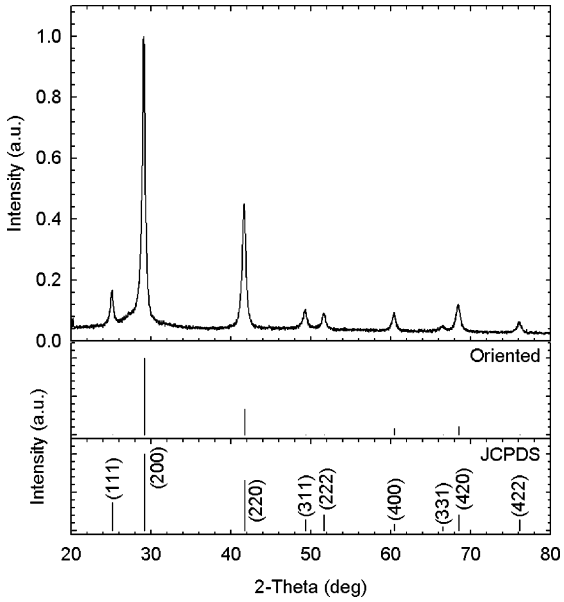

Figure 6. Wide-angle XRD pattern for PbSe NWs. Accompanying stick figures for a randomly oriented JCPDS sample and predictions of a simple texture model are provided.

between neighboring {111} planes on either side of the twin. Both a dashed and a solid line are provided in Figure 5b to aid visualizing this.

Apart from TEM images, the crystallinity of all PbSe NWs is further established by powder X-ray diffraction (XRD) scans (Figure 6). These XRD patterns obtained from various straight/branched NW samples indicate that all NWs exhibit the rock salt structure of PbSe. Theoretical peaks for the PbSe lattice (Figure 6, bottom) correspond well with those obtained from the NWs. Peak broadening is also observed and can be attributed to finite size effects. A Scherrer analysis of the patterns yields sizes in good agreement with direct TEM width measurements.

In Figure 6, several peaks are slightly enhanced or suppressed. This can be attributed to crystallographic texture with a preferred orientation of the NWs lying parallel to the plane of the substrate. For example, both (111) and (220) peaks are suppressed compared to their nominal intensities in isotropically distributed samples. This can be seen by comparing the intensity ratios of the JCPDS pattern to the experimental data. Corroborating this, a simple analysis of texture in the sample suggests that ⟨001⟩-oriented NWs will

Table 1. Calculated Multiplicity Factors for Both Random and Oriented PbSe NWs

reflcn	equiv planes	p_{random}	$p_{oriented}$	$I_{oriented}/I_{oriented(200)}$
{111}	(111), ($\bar{1}$11), (1$\bar{1}$1), (11$\bar{1}$)	4	0	0
{200}	(200), (020), (002)	3	2	1
{220}	(220), (202), (022), ($\bar{2}$20), ($\bar{2}$02), (0$\bar{2}$2)	6	2	0.33
{311}	(311), (1$\bar{3}$1), (11$\bar{3}$), ($\bar{3}$11), ($\bar{1}$31), ($\bar{1}$13), (3,$\bar{1}$1), (1$\bar{3}$1), (1$\bar{1}$3), (31$\bar{1}$), (13$\bar{1}$), (11$\bar{3}$)	12	0	0
{222}	(222), ($\bar{2}$22), (2$\bar{2}$2), (22$\bar{2}$)	4	0	0
{400}	(400), (040), (004)	3	2	0.08
{331}	(331), (313), (133), ($\bar{3}$31), ($\bar{3}$13), ($\bar{1}$33), (3$\bar{3}$1), (3$\bar{1}$3), (1$\bar{3}$3), (33$\bar{1}$), (31$\bar{3}$), (13$\bar{3}$)	12	0	0
{420}	(420), (402), (042), (0$\bar{2}$4), ($\bar{2}$04), ($\bar{2}$40), (4$\bar{2}$0), (40$\bar{2}$), (04$\bar{2}$), (0$\bar{2}$4), ($\bar{2}$04), ($\bar{2}$40)	12	4	0.11
{422}	(422), (242), ($\bar{2}$24), (4$\bar{2}$2), ($\bar{2}$42), ($\bar{2}$24), (4$\bar{2}$2), (2$\bar{4}$2), (2$\bar{2}$4), (42$\bar{2}$), (24$\bar{2}$), (22$\bar{4}$)	12	0	0

have absent the (111), (311), (222), (331), and (422) reflections. Suppression of the (220) as well as the (420) reflection, both relative to (200), is also expected; the (400) reflection is not predicted to change.

This simple analysis of crystallographic texture is conducted by first noting that all factors which affect the relative intensities of XRD lines are independent of preferred orientation, except for the multiplicity factor p. For a specimen with randomly oriented crystals, p accounts for the fact that the probability of a crystal being oriented with a plane {hkl} parallel to the specimen surface is proportional to the number of planes in the {hkl} family. These multiplicities are included as p_{random} in Table 1 ignoring the negatives of the listed planes. If all NWs grow along [001], are randomly oriented with respect to rotation about this axis, and lie flat on the specimen surface, then the only planes which lie parallel to the specimen substrate are those which are members of the [001] zone (i.e. are parallel to [001] and thus have a zero as their third index). Revised multiplicities with these assumptions are listed as $p_{oriented}$ in Table 1.

The predicted intensity of oriented samples is therefore the product of the JCPDS intensity and the ratio $p_{oriented}/p_{random}$ ($I_{oriented} = (p_{oriented}/p_{random})I_{random}$). This value is subsequently normalized to the intensity of the (200) reflection and compared to the experimental data. Resulting intensities are listed in Table 1.

From this analysis, one finds that both the (220) and (420) reflections should be suppressed relative to the (200) reflection. In particular, whereas the normalized intensities of the (220) and (420) reflections are 0.66 and 0.21 in the random JCPDS case, their predicted values for oriented NWs are 0.33 and 0.11. These latter values are in good agreement with the experimental data. Figure 6 includes a stick chart of the predicted intensities and shows that they agree better with the experimental data than with the JCPDS pattern. Furthermore, the (111), (311), (222), (331), and (422) reflections are all suppressed in the experiment. Although the above texture model suggests their complete absence, their appearance here as weak peaks is expected if the wires do not lie perfectly flat on a substrate. Thus, we do not expect quantitative agreement with experiment for the predicted {220}, {400}, and {420} intensities. Along these lines, it should also be noted that, in the case of branched samples, a high incidence of right angles/t-shapes or merge-y NWs will enhance the intensities of the {200}, {400}, and {220} lines compared to an ensemble containing only straight wires. Specifically, right-angles and t-shapes lying flat on a substrate contribute strongly to the {200} and {400} intensities. Likewise merge-y NWs will enhance the {220} peak. This assessment is based on HRTEM images revealing the preferred orientation of these NWs on a substrate. Combined with wires not perfectly flat, these considerations make our predicted intensity ratios somewhat approximate but in reasonable agreement with the experiment.

All NWs possess cylindrical morphologies as opposed to rectangular shapes. This has been demonstrated through field emission scanning electron micrographs (FESEMs) of wires on a tilted substrate (Supporting Information). Cylindrical NW geometries are rationalized by the spherical shape of the NPs used to grow the wires. By contrast, in cases where PbSe nanostructures such as QDs are grown in an uncatalyzed fashion, a cubic shape reflecting the underlying rock salt lattice is often observed.[25,32,34] Additional energy dispersive X-ray (EDXS) spectra of catalyzed NWs show elemental compositions consistent with that of PbSe, 1:1.3 (0.2). A representative EDXS spectrum is provided in the Supporting Information.

Branching Mechanism. Previous investigations of straight and branched CdSe NWs suggest that they grow through a geminate NW nucleation mechanism.[17] A similar growth scheme appears responsible for branching in PbSe NWs. Hence, the geminate growth model likely represents a general scheme for NW branching irrespective of material. As noted earlier, straight wires are formed when Pb is in slight excess of Se, whereas branched wires result when the Pb:Se ratio approaches 4:1. Therefore, provided sufficient quantities of both, two arms can nucleate on the surface of the molten catalyst. If the angle between the two arms is below a critical value ($\theta < \theta_{crit}$), each arm rotates or reorients within (or on) the liquid catalyst to an appropriate orientation that allows them to touch and form a low-energy twin. The result is a merged-y NW with an average $-\alpha\beta$ angle of 70.4° ($\sigma =$ 1.4°) and a complementary angle of 109.5° between {100} planes facing the opposite direction. This is shown in Scheme 1 (left side) along with actual TEM micrographs capturing such structures mid growth. If instead the initial angle between the two arms is greater than the critical angle ($\theta > \theta_{crit}$), the arms have sufficient time during growth to rotate until their mutual angle is approximately 90°. A common rock salt section can then form, locking the two arms into place. Such a scenario is shown on the right in Scheme 1.

While the value of θ_{crit} can be inferred experimentally, by noting both the average and the largest $-\alpha\beta$ angles observed in both PbSe and CdSe merge-y NWs, the critical angle can also be calculated through simple geometric arguments. For example, assuming the radius of each nucleated arm is initially smaller than the catalyst particle (for example, ~80% of the catalyst NP radius), the calculated

Scheme 1. PbSe NW Branching Mechanism

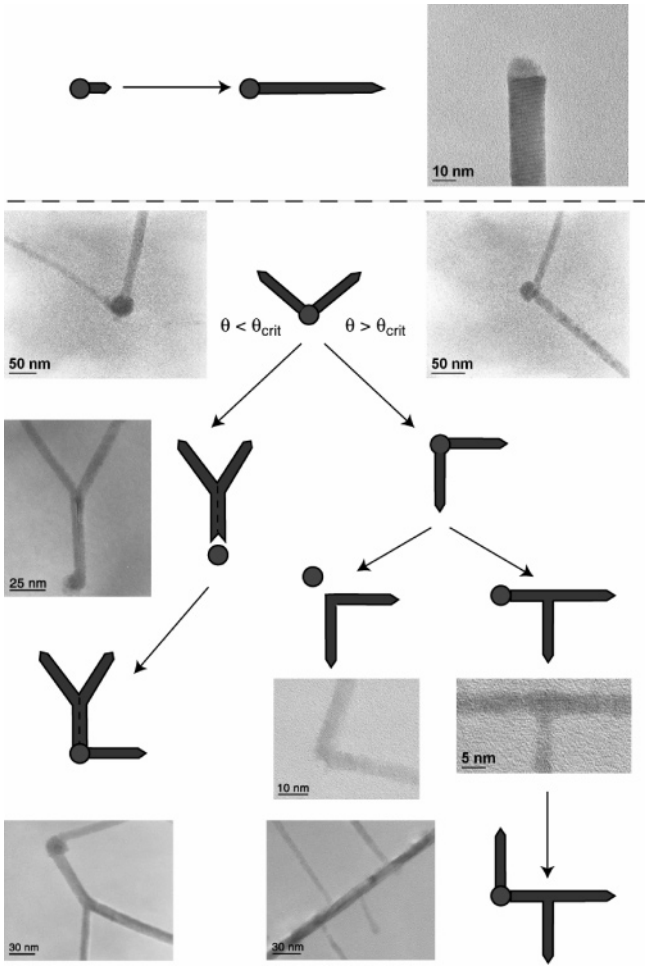

value for θ_{crit} is 77.3°. This corresponds well with overall $-\alpha\beta$ angles of 67.3° ($\sigma = 9.6°$) for *all* merged-y PbSe NWs irrespective of whether a {111} twin plane along γ has been verified by lattice resolved HRTEM images.

Higher Order Nanowires. Higher order PbSe NWs are also observed in branched NW preparations. These structures form when the catalyst particle is retained on the wire after an initial round of branching. Examples can be seen in the lower half of Scheme 1. The geminate NW nucleation mechanism assumes that, under certain circumstances, possibly initiated by changes in the precursor metal-to-chalcogen ratio, multiple NWs can develop on a given catalyst particle during growth. We suggest that the number of nucleated wires is typically two but do not exclude the possibility of more. However, the statistical likelihood of generating three, four, or more arms on a single catalyst particle is thought to be small given the finite size of the NP which, in turn, increases the likelihood that such multiply nucleated arms will coalesce during early stages of the growth. An exception showing three arms arising from a given NP is shown in the Supporting Information.

Figure 7a−d shows four additional examples of higher order structures. True to the underlying rock salt lattice of PbSe, they exhibit 90° angles. Although relatively large, the NWs are typically smaller than their analogous higher order CdSe counterparts.[17] Structures such as in Figure 7b−d appear to be readily explained by a geminate branching

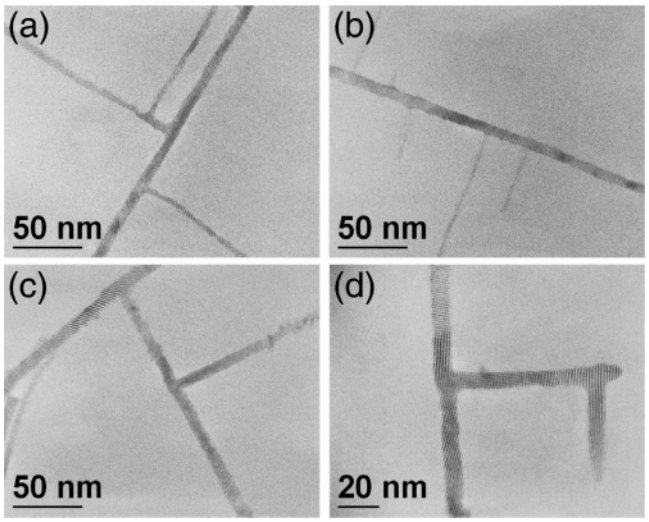

Figure 7. (a−d) Low-resolution TEM micrographs of higher order PbSe NWs.

mechanism where each branching point can be thought of as a location where NW growth is partitioned between two arms, a primary trunk and an emerging sidearm. This step is then followed by continued growth of the main arm. Branching resumes on interruption of this growth by the emergence of a second arm.

At the same time, some branching in higher order structures may not strictly follow a geminate nucleation mechanism. For example, more complex NWs such as that in Figure 7a are difficult to rationalize solely on the basis of a model where only two arms originate from the same catalyst particle at any given time. It appears to be better explained by a scenario where catalyst "fission" can occur. In this picture, the catalyst particle breaks up into multiple fragments, each of which is capable of promoting branched NW growth. Indeed, examples of higher order NWs with multiple catalyst NPs attached to different branches have been observed. A reason such catalyst fission might occur here and not with solution grown CdSe NWs is the presence of NP aggregation. This leads to larger (effective) particles which can break up at a later time. More thorough descriptions of this and other potential branching mechanisms can be found in ref 17.

Another route to higher order structures is a collision mechanism,[17] where the chance encounter between two or more catalyzed NWs leads to branching. This mechanism, though, does not appear to be a major route to branched structures here on the basis of prior experiments. In principle, concentrating the reaction mixture should increase the incidence of branching and also the number of higher order structures. However, we find that increasing the reaction mixture concentration enables the competitive growth of PbSe QDs at the expense of NWs. Furthermore, lattice-resolved HRTEM images indicate that all branching occurs at {100} facets. By contrast, a collision mechanism might predict branching out of non-{100} faces of the lattice, {110} for example.

A final mechanism through which higher order branching can occur involves uncatalyzed growth. In this respect, examples exist in the literature showing uncatalyzed wires

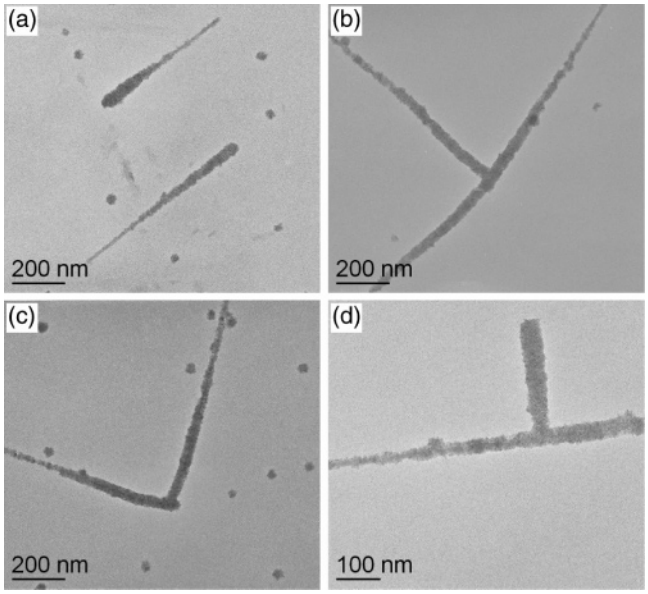

Figure 8. (a−d) Low-resolution TEM micrographs of straight and branched uncatalyzed PbSe wires.

that exhibit branching.[34,35] While control experiments we have conducted also show similar behavior, they also suggest that the primary route to NW growth/branching is catalyzed. Specifically, these experiments indicate a very low incidence of uncatalyzed NW growth with the majority species in such experiments consisting of irregular spherical PbSe aggregates rather than wires.

Uncatalyzed Growth. Control experiments conducted under the same conditions as (catalyzed) straight/branched NW preparations indicate a small incidence of uncatalyzed growth in the absence of Au/Bi NPs. These wires have noticeably different morphologies than catalyzed NWs. Namely, they have a polycrystalline structure composed of smaller spherical PbSe aggregates. Examples can be seen in Figure 8 where both straight (Figure 8a) and "branched" (Figure 8b−d) uncatalyzed wires are shown. Additional TEM micrographs are provided in the Supporting Information.

In all cases, the bulk of the uncatalyzed sample consists of spherical PbSe aggregates which lie adjacent to the wires in Figure 8a,c. Such aggregates have previously been observed and are thought to assemble into a NW by aligning in solution through dipole−dipole interactions.[34,35] The origin of this dipole has very recently been suggested as arising from various configurations for the stoichiometric termination of polar {111} faces.[35] In certain arrangements, Pb and Se termination of {111} faces induces a net dipole along ⟨100⟩. This explanation is thus general and may explain previous observations of nanocrystal alignment.[34,40] EDXS analyses of the uncatalyzed wires indicate that they are PbSe with a Pb:Se stoichiometry of 1:1.1(0.2). Local EDXS spectra have also been taken along the NW length to verify the uniformity of the elemental composition. Examples are provided in the Supporting Information.

Distinguishing catalyzed from uncatalyzed NWs are the following features which enable us to conclude that the primary branching mechanism in the current synthesis is catalyzed. Specifically, catalyzed NWs generally have a Au/Bi NP attached to one end, providing evidence for a seeded growth mechanism. Representative TEM images of NWs are provided in the Supporting Information. The surfaces of catalyzed NWs are also smooth with little roughness. This has been confirmed by measurements of NW diameter fluctuations, yielding intrawire variations of 7(3)%. By contrast, width fluctuations of uncatalyzed NWs can be as large as the full diameter of the wire. In addition, the catalyzed NWs are single crystals (Figures 1−4) whereas HRTEM images of uncatalyzed wires reveal them to be polycrystalline, identical with previous observations.[34] Furthermore, the widths of the catalyzed NWs are more closely associated with the initial diameters of the Au/Bi NPs despite their apparent growth in solution. This should be contrasted to the size of uncatalyzed NWs which have average diameters of 38(12) nm. Along these lines, the uncatalyzed NWs are almost always strongly tapered (Figure 8a) whereas the catalyzed wires are not (Figure 1). Finally, a major distinction between catalyzed and uncatalyzed growth is the absence of any merge-y's in preparations based on the latter scheme. In this respect, just as merged-y nanostructures were characteristic of a geminate NW nucleation mechanism, they also appear to be a unique signature of catalyzed growth. As such, we conclude that induced branching in PbSe NWs occurs through a catalyst-mediated mechanism.

Conclusions

The successful solution-based synthesis of confined PbSe NWs has been demonstrated for both straight and branched NWs. This work provides one of the first examples of self-induced branching in NWs and addresses an emerging need for shape control in 1D materials. A qualitative scheme developed to explain this behavior suggests that branching observed in both CdSe and PbSe NWs follows a general mechanism which is potentially applicable to other systems. This, in turn, provides a method for creating nanostructures of varying morphology. As such, the work is relevant to improving our understanding about the evolution of mesoscopic optical, electrical, and physical properties with size, shape, and dimensionality. Furthermore, in addition to being of interest for basic science reasons, such straight and branched NWs may also have potential device applications.

Acknowledgment. We thank the University of Notre Dame, the Notre Dame Faculty Research Program, the Notre Dame Radiation Laboratory, and the Office of Basic Energy Sciences of the U.S. Department of Energy for financial support and for use of their facilities. K.L.H also thanks the ICDD for the Ludo Frevel Crystallography Scholarship. We also thank A. Khandelwal for assistance with FESEM measurements.

Supporting Information Available: Low- and high-resolution TEM micrographs of straight PbSe NWs, TEM micrographs of straight and branched NWs with attached catalyst NPs, TEM micrographs used for NW sizing, HRTEM micrographs of additional merge-y structures, FESEM micrographs of PbSe NWs on a tilted substrate, an EDXS spectrum of uncatalyzed NWs, low-resolution TEM micrographs of uncatalyzed NWs, and EDXS spectra of uncatalyzed straight/branched PbSe NWs. This material is available free of charge via the Internet at http://pubs.acs.org.

(40) Tang, Z. Y.; Kotov, N. A.; Giersig, M. *Science* **2002**, *297*, 237.

CM050952+